Regional Photovoltaic Power Fluctuations within Time Frames of Frequency Regulation Controls: A Study with High Resolution Data

Joao Gari da Silva Fonseca Junior[a*], Yuki Nishitsuji[a], Yusuke Udagawa[a], Chiyori T. Urabe[a], Tetsuo Saito[a], Fumichika Uno[b], Hideaki Ohtake[b], Takashi Oozeki[b], Kazuhiko Ogimoto[a]

[a] Collaborative Research Center for Energy Engineering, Institute of Industrial Science (IIS), University of Tokyo, 153-8505 Komaba 4-6-1, Meguro-ku, Tokyo, JAPAN. E-mail: jfonseca@iis.u-tokyo.ac.jp

[b] System and Applications Team, Research Center for Photovoltaic Technologies, National Institute of Advanced Industrial Science and Technology, AIST Tsukuba Central 2, 305-8568 Tsukuba, Ibaraki, JAPAN.

Abstract: The growth of renewable energy penetration on power grids is reaching high levels in many countries around the world. In such high penetration scenarios, the proper characterization of the intermittency of renewable power generation becomes important to the stable operation of power grids. In this study, using the most recent high resolution GHI data in Japan, we characterize short-term fluctuations of photovoltaic, PV, power in regional scale, in a scenario of high penetration of PV. We analyzed 1 year of data with a resolution of 10 seconds for the Kanto area in Japan. The results show that the distribution of the short-term fluctuations are non-Gaussian, presenting a shape similar to a Laplacian distribution. In addition to statistical aspects, a methodology is presented to evaluate the fluctuations considering aspects relevant to power grid operators. Applying this methodology, we show, for example, that the highest short-term fluctuations within the time frame of secondary regulation control of frequency of a regional power system reached 5% of the power demand of the hours in which they occurred. Fluctuations of PV power within primary regulation control time frame were within 3% of power demand and the 99th percentile of the fluctuations were well within 1% of it. With the proposed methodology, which can be generally applied, we go beyond description of the statistical properties of the short-term fluctuations of PV and show the importance to evaluate them in a context relevant to power grid operators, considering season, weather, and power demand aspects.

Keywords: Photovoltaics, Regional Power Generation, Short-term Fluctuations, Power systems, Frequency Regulation Control Time Frames

1. Introduction

The number of installations of photovoltaic, PV, systems in markets around the world has been growing exponentially since 2006 [1]. According to the IEA, just in 2015, additional PV installed capacity reached more than 50 GW [1]. Japan has been an important part of this growth with an additional installed capacity of PV in 2015 of almost 11 GW, reaching a total amount of 34 GW of PV (a 7-fold increase since July of 2012). Nevertheless, in the case of Japan, there are concerns about the sustainability of further growth of PV, as it has been concentrated in areas with low power demand and cheap land. To mitigate such concerns, it is critical to identify properly and to anticipate the impact of high penetration of PV power on current power grids. In this regard, one pressing issue is the characterization of fluctuations of PV power generation in large scale due to weather changes.

Fluctuation of PV power output has been studied in many countries [2]. Many studies are focused on the analysis of the output as a signal and on formulations to describe it. For example, Wienken et al. studied the combined output of 100 PV systems in Germany, with resolution of 5 minutes, and verified how much of the short-term fluctuation of single systems' output is reduced compared with the total output of the ensemble [3]. Otani et al. studied local solar irradiance fluctuations in Japan (which affect directly PV power) of 9 weather stations in a grid measuring 4 km x 4 km, analyzing individual and total 1-minute output. The authors quantified fluctuation factor and power spectral density of the ensemble and single stations [4]. In the U.S., Jewell and Unruh studied the limits on cloud-induced fluctuation on PV systems, simulating PV power generation based on 1-minute resolution solar irradiance measured in a single location [5]. The authors extended the study to include different levels of PV power penetration scenarios in regional scale, estimating their effects on the operation of a power grid, and estimating maximum allowable PV penetration for the area of a large power utility in the state of Kansas in the U.S. Recent studies have benefited of the availability of different and extensive sources of data. For example, Murata et al. studied 1 minute data of 3 months of 52 PV systems in Japan in 3 areas of the main island Honshu [6]. With this data, the authors derived equations to predict geographical correlation between fluctuations of PV systems dispersed in a region. Woyte et al. focused on spectral analysis of PV power fluctuations and their effects on distribution networks [7]. Using 1 year of 5 seconds irradiance data from Belgium, the authors simulated how residential PV power fluctuations would affect distributed power grids and described PV power fluctuations in the nodes of a grid using a mathematical model based on the Haar wavelet transform. Curtright and Apt [8], showed the benefits of power spectral analysis to characterize PV power fluctuations. Using 10 seconds and 1 minute data of 4 PV power plants in 2 locations in Arizona, U.S., the authors showed that PV power fluctuations may be more intermittent than wind. Focusing on the high frequency components of solar irradiance fluctuations and how it generates ramps of PV power, Lave et al., analyzed clearness index data with 1 second of resolution in 6 locations near each other in San Diego, U.S. [9]. The authors performed a wavelet decomposition to analyze the fluctuations, characterized them statistically, and found good level of agreement between their results and the model developed by Hoff and Perez [10]. Still on ramps, Wellby and Engerer [11], categorized cloud phenomena and weather phenomena associated with ramps of PV power in the Australian Capital Territory. They showed that most positive ramps were caused by cloud bands and fog dissipation, and that negative ramps were often caused by passage of cold fronts in the area studied. In Spain, geographical dispersion of PV systems and maximum fluctuation were also studied by Marcos et. al, who used 1 second data of 7 PV power plants to verify the level of smoothing that occurs in PV power fluctuations in a 1000 km^2 area [12]. The authors evaluated PV power fluctuations in different temporal resolutions and estimated maximum fluctuations that can occur for an arbitrary number of PV power plants applying an empirical model they developed previously [13]. Kato et al. analyzed changes in the fluctuation of solar irradiance according to geographical dispersion [14]. Using solar irradiance measured in 61 locations in the central area of Japan, they applied the empirical model of Nagoya et al. [15] to calculate spatial average solar irradiance considering smoothing effect. Finally, Anvari et al. evaluated PV power and wind power fluctuations in databases with different temporal resolutions, different collection periods, and of 8 different locations in the world [16]. The authors performed a thorough statistical analysis, characterizing multiple types of variability and non-linearity of solar and wind power generation.

Often, analyses as those described focus on the fluctuations of a few data collection points, or on periods of data collection shorter than a year. Furthermore, many studies focus on the description of the fluctuations of power and frequency themselves and on trying to model them with empirical equations. Studies going beyond that and examine, for example, when and which fluctuations should be a cause for concern to a power grid operator are still exiguous. For example, power grid operators are often interested in short-term fluctuations that happen within the time frames of their primary and secondary regulation controls of frequency. If PV power fluctuates strongly in a short period of time in a given power grid for example, depending on the size of such fluctuation, it might not be possible to avoid sudden drops or surge of frequency and voltage, which may affect the balance of power demand and supply, and even the proper operation of other power generators connected to such a grid.

In this study, we apply 1 year of one of the most recent measurements of solar irradiance in regional scale and high temporal resolution done in Japan in the analysis of short-term fluctuations of PV power. The data used are a subset of the national project called PV 300, conducted by the Ministry of Economy, Trade and Industry o Japan, METI. This subset contains one year of 10 second measurements of solar irradiance for 60 stations covering the area of Kanto region in Japan and surroundings (an area of more than 32430 km^2).

With these measured data, we simulate and analyze one year of regional PV power generation in a scenario of high penetration of PV. The objective is to present a comprehensive characterization of short-term PV power fluctuations in regional scale. To do that, we use a methodology to study short-term fluctuations of PV considering power demand on the grid, season, and weather conditions at the time of the fluctuations. The analysis is focused on fluctuations of PV power that happen within the time frames of primary and secondary power and frequency regulation controls of power systems. In this way, we go beyond simple evaluations of PV power fluctuations in isolated fashion available in literature, and approach the problem from a context that is relevant to power grid operators, so that the impact of high penetration of PV power on current power grids can be better understood.

2. Description of the Data Set

The data set used in the study is a subset of a national database of global horizontal irradiance, GHI, measurements called PV 300. The PV 300 database was organized within the framework of the Project for Power Stabilization at the Mass Introduction of New Energy. This project is sponsored by the Ministry of Economy, Trade and Industry in Japan, METI, and started in 2009. In this project, GHI is continuously measured in high temporal resolution in 321 points spread throughout the Japanese territory. Each one of the 10 power utilities in Japan is in charge of guaranteeing the quality and accuracy of the measurements done in locations within their operation area. Furthermore, they are also in charge of the maintenance of the equipments used in the measurements and of the management of the data acquired.

This study is focused on the Tokyo Electric Power Company, TEPCO, operation area in Japan (Fig. 1). This operation area comprises the whole Kanto region which comprises Tokyo, Kanagawa, Chiba, Saitama, Tochigi, Ibaraki, and Gunma prefectures. Besides Kanto, TEPCO operation area also includes the Yamanashi prefecture and part of Shizuoka prefecture (also in Fig. 1). However, for brevity, we refer to target operation area in the text as the Kanto area.

This operation area was chosen for a few reasons. First, it has the highest national power demand consumption. It also has one of the greatest potentials for new installations of PV systems in Japan. Finally, using the real area operated by a power utility as target, a realistic assessment of the PV power fluctuations that a utility has to deal with in a scenario of high penetration can be provided.

Data from 60 GHI measurement points of the PV 300 database within Kanto area were used. The approximate location of the measurement points and the operation area are in the map in Fig. 1. To capture the variety of conditions in which PV systems can be installed in the target area, the pyranometers used in the GHI measurements were installed in several locations, including plain areas, scarcely and densely populated areas, areas in which one or more directions towards the horizon have high or low mountains, or forests nearby, and so on. Most of the pyranometers are installed on top of non-residential buildings. The buildings are located in residential and non-residential areas. All measurement stations had at least one thermopile pyranometer to measure GHI, and a few locations also had an extra photodiode based pyranometer and extra pyranometers used to measure tilted irradiance.

The period of the measurements used in the analyses is one year, from November 2015 to October 2016. Within this period, measurements of GHI were done with a resolution of 10 seconds

(0.1 Hz). Every month, the quality of the data measured in each station was checked for consistency, and faulty data were excluded from the data set used in the analysis.

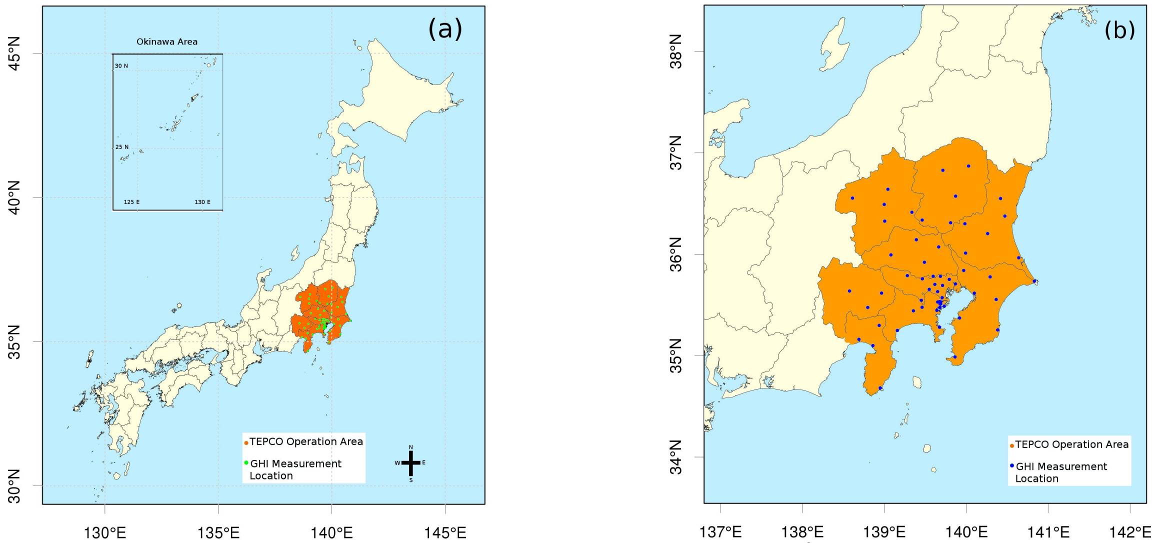

*Both maps were built with the maptools R library and data publicly available from the GADM database.

Figure 1- Japan map (a) and target area of the study (b) with GHI measurement locations.

3. Methodology

To characterize short-term fluctuations of PV power in 10-second temporal resolution and regional scale, the GHI measured in the 60 locations of the target area were converted to the equivalent PV power that they would yield in regional scale. To do that, the modeling described in Subsection 3.1 was used with the simulation conditions described in Subsection 3.2. Once regional PV power output was calculated, its short fluctuations were analyzed according to different time frames. In this case, short-term fluctuations were estimated using the method described in Subsection 3.3.

3.1. Regional Photovoltaic Power Output Modeling

We used the method proposed by Oozeki et al. [17] to estimate regional PV power output based on GHI point measurements. In this section, a brief explanation about the model is provided. The method works with several layers with different kinds of information regarding PV systems, landscape, and buildings of the target region. The set of layers provide the necessary information to characterize the potential of the region to generate PV power. Based on the information provided by the layers, a weighted averaging procedure is applied on GHI measurement points to obtain the equivalent irradiance that can be converted to PV power in a final step. The application of the method follows the steps showed in Fig. 2.

Once the equivalent solar irradiance that can be converted to PV power in step 5 of Fig. 2 is calculated for each area of the Voronoi diagram in step 1 of the same figure, the regional yield is determined. This value is then used to estimate how much PV power will be generated at the region. These calculations are done for each time in which GHI was measured within the target period (10 seconds measurements for 1 year). The final conversion from solar irradiance to PV power is based on a formulation suggested by the JISC8907 standard to calculate PV power from solar irradiance.

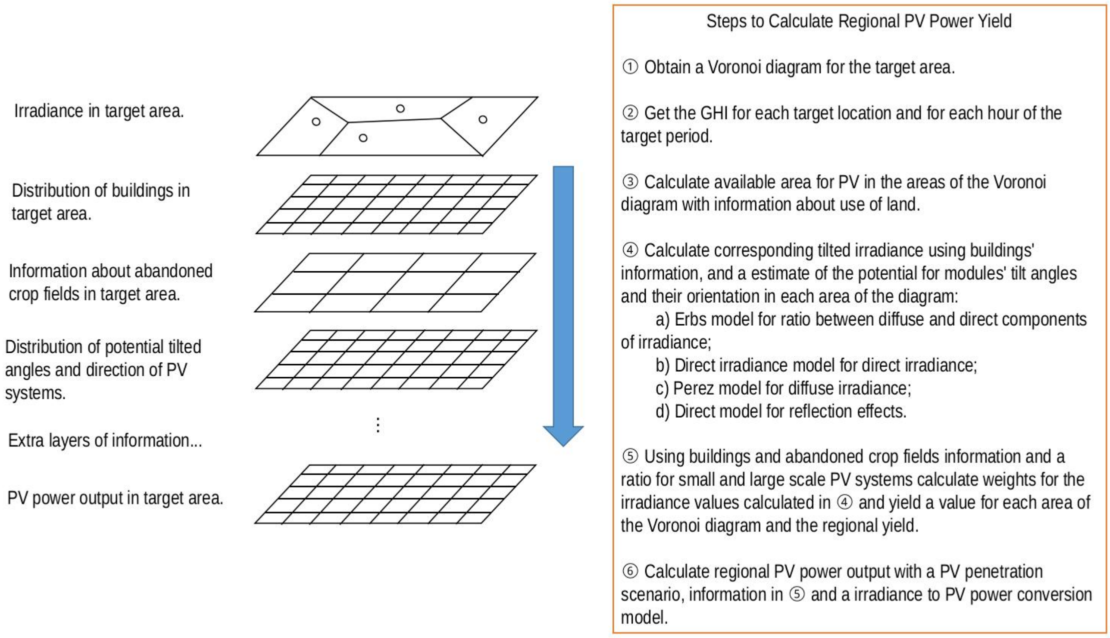

Figure 2- Method to estimate regional PV power from point measurements of GHI.

In this formulation all the non-linearities involved in the conversion process are regarded in a single parameter called performance ratio. In this fashion, the PV power output yielded in the target region is calculated as shown in Eq. 1.

$$E_p = P_{AS} \cdot \frac{H_{AG}}{G_s} \cdot K \qquad (1)$$

In Eq. 1, E_p is the PV power output in kW; K is the performance ratio; P_{AS} is the total installed rated power in kW. Variable H_{AG} is the equivalent average irradiance reaching the modules calculated in step 5 of Fig. 2, in kW/m^2, and G_s is the irradiance in standard conditions, regarded as 1 kW/m^2.

It should be noted that if more information were available, a more complex conversion model could be used to estimate PV power output from solar irradiance. For example, considering distributions of PV systems IV curves, performance dependence on module temperature, different atmospheric conditions, soiling effects, spectral mismatches, degradation rate, etc., arguably a more accurate estimate of PV power than the one Eq. 1 yields could be provided. Nevertheless, as the required information for such complex conversion model is not available, the study focused on short-term fluctuations of PV power and not in its absolute yield, the conversion approach in Eq. 1 was employed.

3.2. Model Configuration Parameters and Simulation Conditions

The geographical information necessary to map the target area, shown in Subsection 3.1, were obtained from Japanese GIS related sources [18], [19]. Required information about density and types of constructions, as well as abandoned crop fields, according to their location in Kanto area in Japan, were retrieved from government statistics databases [20]. Finally, information regarding the potential for PV systems installations, their modules’ distribution of tilt angles and orientation according to the prefectures in the target area were provided by the National Institute of Advanced Industrial Science and Technology, AIST. This information comes from a consolidated database of the AIST, which contains series of monitoring and survey data regarding PV installations in Japan. Example of these surveys are also available in Oozeki et al [17].

Regarding parameter K in Eq. 1, it was set to 0.8 as, according to a guideline of the Japanese Photovoltaic Energy Association [21], for Japan losses between 20% to 30% in the conversion process can be expected when estimating PV power output. In the same Eq. 1, a scenario for the installed capacity has to be assumed to set parameter P_{AS}. To characterize such scenario, a study published by NEDO with scenarios of PV power penetration for 2030 in Japan was used [22]. The scenario chosen from this study was one in which the national PV power installed capacity in 2030 reaches 53 GW. To determine the amount corresponding to TEPCO area, it was further assumed that in each region, the PV systems installed capacity will be proportional to the ratio between the region and the national annual power demand (which has been gradually returning to values of 2010, after dropping sharply soon after the nuclear disaster in Fukushima). Following such assumptions, 17.5 GW of PV power would be installed in the area currently operated by TEPCO by 2030. Thus, P_{AS} in Eq. 1 was set to 17.5 GW.

3.3. Short-term Fluctuations within the Range of Primary and Secondary Frequency Regulation Controls

Once 10-second resolution PV power output in regional scale was estimated throughout one year, its fluctuations were analyzed. To deal with short-term frequency instabilities in the power grid, operators use what is known as primary and secondary frequency regulation controls. In Japan, primary regulation control is done using autonomous governor free control, GFC, applied by each turbine of thermal and hydro power plants**.** Secondary regulation control is usually performed with centralized load frequency control, LFC, on the turbines of power plants. For Japanese power utilities, the time frame of GFC is in the order of seconds up to 1 minute, and for the LFC the time frame varies between 1 minute to 30 minutes [23]. Thus, the analysis was carried out focusing on fluctuations of PV power that happen within those time frames.

In reality, depending on the size of the frequency variation and available regulation reserves, LFC can be applied in time frames that overlap the time frame of GFC. However, to analyze the PV power fluctuations, a clear distinction between the time frames was assumed.

To isolate different components of the 10-second regional PV power output according to the time frame of primary and secondary regulation controls, we applied the decomposition method recommended by the Institute of Electrical Engineers of Japan [23], with the modifications proposed by Urabe et al. [24] to distinguish fluctuations related with the GFC time frame from those related with the LFC time frame. For the GFC, first a reference to which compare the PV power output is set. This reference is regarded as the 1 minute moving average of the output as shown in Eq. 2. Once the reference is set, it is extracted from the output so that only fluctuations within 1 minute are left, Eq. 3.

$$P_{1min.}(k) = \frac{1}{N}\sum_{i=t-30s}^{t+30s} P_{PV}(i) \tag{2}$$

$$\Delta P_{GFC}(k) = P_{PV}(k) - P_{1min.}(k) \tag{3}$$

In Eq. 2, $P_{1min.}$ is the 1 minute moving average of the PV power output for the time stamp of point k, in kW; P_{PV} is the 10-second resolution PV power output, in kW. Variable N is the total number of 10 second measurements within the period t-30 seconds to t+30 seconds centered on the time stamp of point k. Finally, in Eq. 3, ΔP_{GFC} is PV power output fluctuation, in kW, related to or within the time frame of GFC.

The PV power fluctuation within LFC time frame was calculated in the same fashion, although the reference in this case is based on 30-minute averages as shown in Eq. 4. This is done to exclude long period fluctuations from the analysis. Furthermore, PV power output fluctuations within the time frame of GFC are also excluded from fluctuations within LFC time frame as indicated in Eq. 5, which yields Eq. 6.

$$P_{30min.}\ k\ = \frac{1}{M} \sum_{i=t\ \ 15min}^{t+15min} P_{pv}\ i \tag{4}$$

$$\Delta P_{LFC}\ k\ = P_{PV}\ k \quad P_{30min.}\ k \quad \Delta P_{GFC}\ k \tag{5}$$

$$= P_{1min.}\ k \quad P_{30min.}\ k \tag{6}$$

In Eq. 4, $P_{30min.}$ is the 30-minute moving average of PV power output, in kW. In Eq. 5 and Eq. 6, ΔP_{LFC} is PV power output fluctuation, in kW, related to or within the time frame of LFC. Variable M is the total number of 10 second measurements within the period t-15 minutes to t+15 minutes centered on the time stamp of point k. With this methodology, we isolated different components of the regional PV power output, so that just fluctuations related with the time frames of primary and secondary power and frequency regulation controls could be identified. Fluctuations of PV power happening within these 2 time frames are regarded here as short-term fluctuations.

4. Results

The results obtained are presented in the next 3 subsections. In Subsection 4.1, the regional PV power output fluctuations are characterized regarding their distribution and frequency. For a power grid operator, it is not only important to know what kind of fluctuations occur and their magnitude, but also in which weather and power demand conditions they happen. An analysis from this point of view is presented in Subsection 4.2. In Subsection 4.3 we complement the analysis of Subsection 4.2 characterizing the conditions that yielded 3 examples of extreme fluctuations of regional PV power.

4.1. Characteristics of Short-term Fluctuations of Regional PV Power

The duration curves showing the frequency and magnitude of PV fluctuations within the time frames of LFC and GFC in 1 year are in Fig. 3(a) and Fig. 3(b). A gap was inserted in the plot to exclude night periods and to focus the analysis on extreme values.

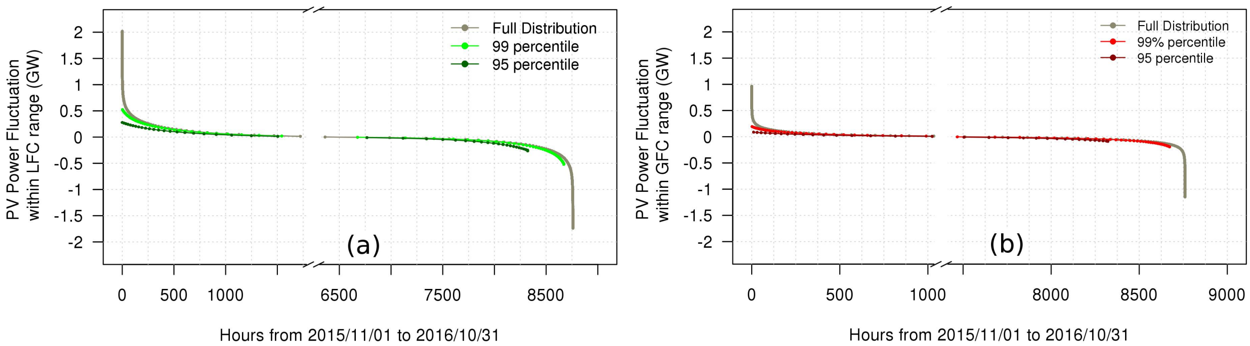

Figure 3- Duration curve of regional PV power fluctuations within the time frame of LFC (a) and GFC (b) excluding night periods (indicated by the gap).

Regional PV power fluctuations within the LFC time frame had a maximum value of 2 GW and a minimum value of -1.7 GW. Nevertheless, the frequency of such extreme fluctuations was low. The 99 percentile line in Fig. 3(a) shows that most of the fluctuations are within -0.5 GW and 0.5 GW. Thus, considering that the minimum power demand of Kanto area in the period studied was near to 20 GW, the worst possible case regarding occurrence of extreme values suggests that only in 1% of the period studied PV output fluctuations would have a value between 2.5% and 10% of power demand. In the rest of the year, the value would be lower than 2.5%. Still, as such fluctuations occurred within the LFC time frame, even if seldom, they would still present a substantial challenge to a power utility having to deal with them.

The duration curve of PV power fluctuations within the time frame of GFC are presented in Fig. 3(b). Extreme values in this case were approximately half of the extreme fluctuations within the LFC time frame, with values of -0.96 GW and +1.15 GW. The 99 percentile of the fluctuations, shown in Fig. 3(b), had values ranging between -0.19 GW and +0.19 GW. These values are also substantially lower than those found for fluctuations within the LFC time frame. Nevertheless, such fluctuations can be regarded as even more difficult to deal with, than those within LFC time frame, as they occurred in less than 1 minute.

In Fig. 4, the shape and extension of the frequency of both kinds of fluctuations, expressed in units of each distribution’s standard deviation, are presented. Confirming the trend noted in Fig. 3, fluctuations within GFC time frame are stronger than those related with the LFC time frame. In this case, extreme fluctuations within LFC time frame had extended up to 12 times their standard deviation, whereas those within GFC time frame extended up to almost 20 times their standard deviation. Disregarding extreme negative and positive outliers (the fist and last points in each distribution in Fig. 4), the same trend remains.

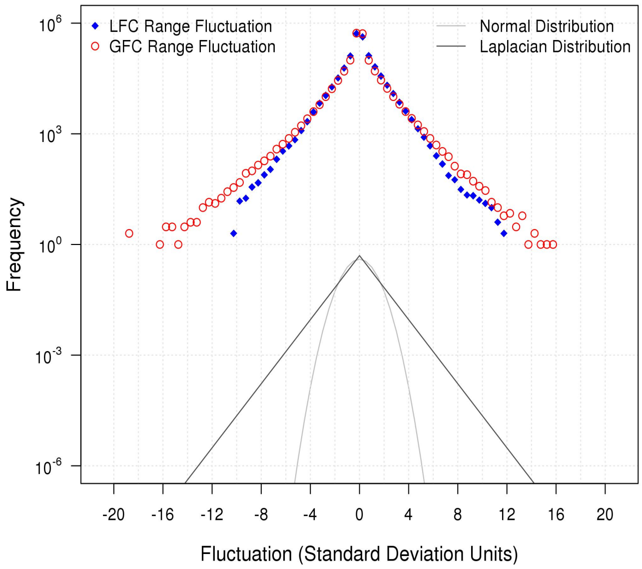

Figure 4- Frequency of the short-term regional PV power output fluctuations in 1 year.

As also shown in previous studies [13], [16], the fluctuations of regional PV power denote a high degree of symmetry, which can be related with transitory weather phenomena. Regarding the shape of both distributions, they are non-Gaussian, presenting heavy tails and a general shape more similar to the shape of a Laplacian distribution shown in Fig. 4. Thus, applying Gaussian assumption in this case would yield serious underestimations of the variability, in short-term, of the regional PV power output in a future power grid circumstance of smaller synchronous inertia.

4.2. Characteristics of the Conditions in which the Short-term Fluctuations Occurred

The effect of the season on the fluctuations during the period studied is presented in Fig. 5(a) and Fig. 5(b). In Fig. 5(a), one can see a strong seasonal effect on the largest fluctuations of PV power within the LFC time frame. The highest fluctuations in this case happened in summer season in Japan. They reached their highest positive value during the month of August, and the highest negative value in July. The 99th and 95th percentiles of the fluctuations in Fig. 5(a) provide a better understanding of the seasonal trends. The percentiles' magnitude generally increased with the change of season from winter to summer, reaching peak values in August. For example, in the case of the 99th percentiles, in absolute values, it increased almost 2 times, from 0.5 GW in November of 2015 to approximately 1 GW in August of 2016. This behavior is related with the weather characteristics in Kanto from June to August. From June to July there is a rainy season, causing sudden changes in the atmospheric conditions of the area. In August, instabilities were caused by frequent passage of typhoons and also by the fact that summer in Japan is humid with high concentration of water vapor, which facilitates cloud formation.

Regarding the fluctuations of power within the GFC time frame in Fig 5(b), although their magnitude are near half the size of those in Fig. 5(a), they also varied according to the season. In this case, the 99th percentile of the fluctuations, in absolute values, increased from 0.15 GW to 0.3 GW. On the other hand, the highest fluctuations of power within GFC time frame did not increase gradually with the change from winter to spring and to summer, as it happened in the LFC time frame case. In winter, they had consistently values around 0.5 GW, and in the rest of the year the highest absolute values varied from 0.5 GW to 1.2 GW.

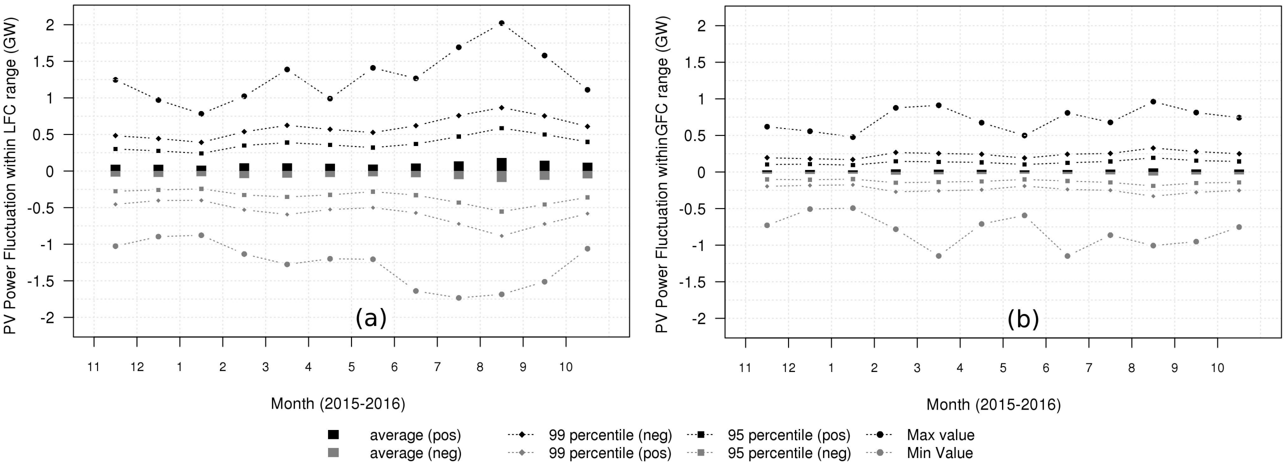

Figure 5- Monthly distribution of fluctuations within LFC (a) and GFC time frame (b) of regional PV power output.

The characteristics of the PV power fluctuations according to the atmospheric conditions in which they happen, are also important information to power grid operators. Such information is in Fig. 6(a) and Fig. 6(b), which contain the magnitude of the fluctuations according to the 30-minute average clearness index of the moment in which they happened. The average clearness index was used so that the general condition at the time of the fluctuations could be better represented. It was calculated using the average irradiance that reaches the PV panels described in Subsection 3.1.

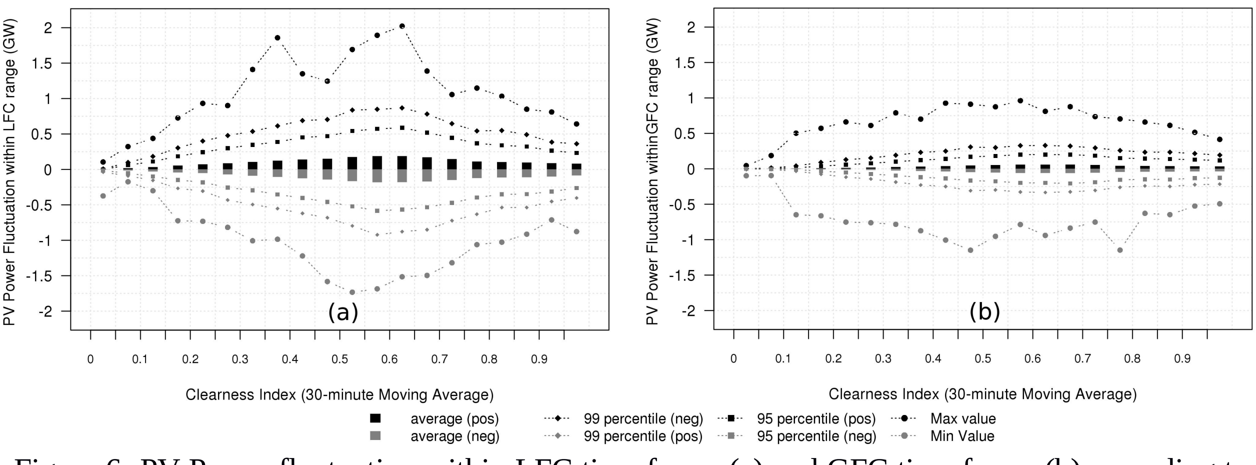

Figure 6- PV Power fluctuation within LFC time frame (a) and GFC time frame (b) according to clearness index (1-year period).

The results in Fig. 6(a) indicate that, annually, the highest PV power fluctuations within LFC time frame happened with average clearness index values ranging between 0.5 and 0.65. Such values represent partially cloudy sky. Clearness index values higher than 0.65 represent skies with fewer clouds and in this case there was a continuous drop of the magnitude of the fluctuations with the increase of the clearness index. The same happened when the clearness index decreased to values below 0.5, and the sky became cloudier until reaching overcast conditions. Looking at the 99th percentiles in Fig. 6(a), its highest absolute values were slightly below 1 GW. In contrast, the highest fluctuations' values were considerably higher (near to 2 times) reaching 2 GW in the period studied. These results show that throughout the year, there are a few occasions when PV power fluctuations achieve values that are completely outside their usual range. Moreover, such fluctuations will occur in a variety of atmospheric conditions. In a scenario with high penetration of PV power, identification of those cases is of critical importance to the stable operation of power grids.

The percentiles of the GFC time frame related fluctuations of power in Fig. 6(b) presented similar behavior to those of within the LFC time frame in Fig. 6(a). The magnitude of the 99th and 95th percentiles' fluctuations reached their peak absolute values when the clearness index was between 0.6 and 0.65 (0.3 GW and 0.2 GW) respectively. Regarding the highest fluctuations of PV power within GFC time frame, 2 distinct characteristics are noted in Fig. 6(b). Firstly, there was not a specific short range of clearness index values (as in the case of the LFC) in which the highest fluctuations occurred. The highest GFC time frame related fluctuations of power reached values near to 1 GW and such values occurred with clearness index values as low as 0.41 and as high as 0.7. Secondly, in the GFC time frame the highest fluctuations of PV power according to the clearness index were more than 3 times higher than those of the 99th percentiles. These results reinforce the trend noted in Fig. 4, regarding outliers values. Thus, extreme fluctuations within the GFC time frame can happen in a wider variety of weather conditions than in the LFC time frame; and when they happen there is an even stronger difference between usual and extreme fluctuations of PV power than there is within the LFC time frame.

The power demand conditions in which short-term fluctuations of PV power happened are also important. The reason is that, often, daily operational reserves in a power system are pre-allocated according to the expected power demand. In Fig. 7(a) and Fig. 7(b), PV power fluctuations within LFC and GFC time frames are plotted against the respective average power demand of the hour in which they happened.

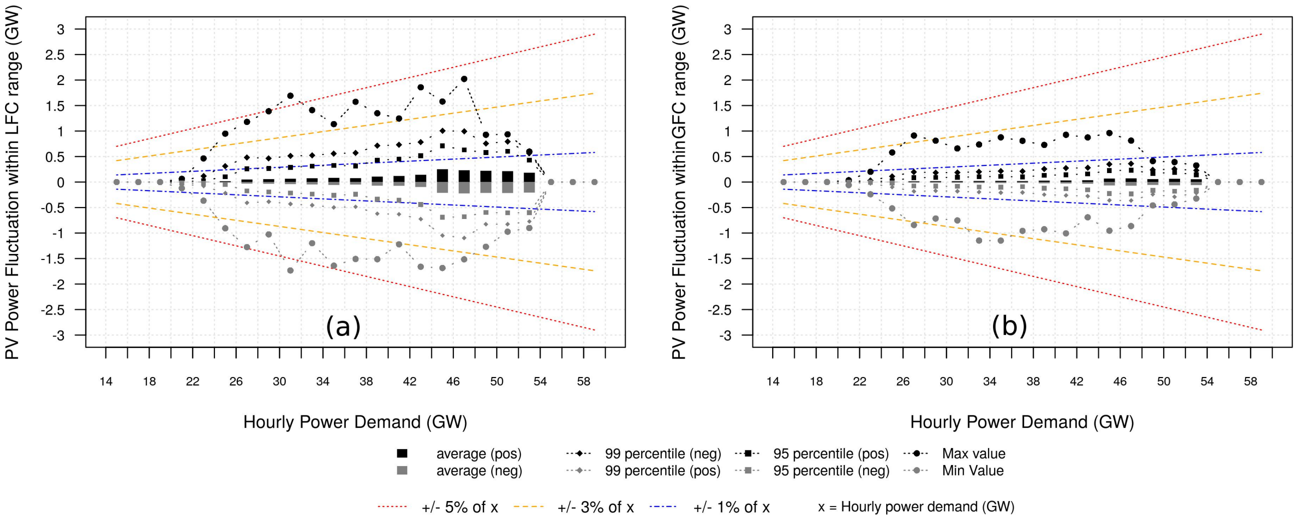

Figure 7- PV Power fluctuation within LFC time frame (a) and GFC time frame (b) according to average daily demand of power (1-year period).

Based on the results in Fig. 7(a), the highest PV power fluctuations within the LFC time frame had values near to 5% of the average power demand of the hour in which they occurred in the worst case. Additionally, extreme fluctuations of PV power higher than 1 GW can occur in wide range of power demand values, from 26 GW to 48 GW. Regarding the percentiles, 99 percent of PV power fluctuations within LFC time frame would be well within -3% and 3% of the respective power demand, and 95% of them would be near to -1% and 1% of their respective power demand. Furthermore, still looking at the 99th and 95th percentiles, in general, there is a relation between the size of the fluctuations of PV power and power demand. In general, and throughout the year, days with high power demand often were also days with high PV power fluctuations. This is explained by the fact that in Kanto area, the highest power demand in the year happens in summer, which is also season with unstable weather, which affects PV power generation. In the case of GFC time frame in Fig. 7(b), a similar trend is observed regarding the increase of the fluctuations with the average power demand of the hour in which they happened. In this case however, peak values of the fluctuations were within -3% and 3% of the respective power demand, and both studied percentiles were well within -1% and 1% of the same parameter.

The consequence of this relation between PV power fluctuations and demand regardless of the fluctuations' time frame, is that, often, high PV power fluctuations tend to occur in days when large amounts of operational power reserve would be allocated anyway regardless of the level of PV power penetration in the grid. Therefore, in the case of Kanto area, the relation between PV power short-term fluctuation and power demand supports high penetration of PV power in the grid.

4.3. Analysis of 3 Examples of High Fluctuation of PV Power

To clarify the connection between extreme fluctuations of PV power noted in subsections 4.2 and 4.3 and the weather conditions that generated them, in this subsection 3 examples of extreme fluctuations of PV power are discussed.

In Fig. 8 and Fig. 9 are the PV power generation and corresponding satellite visible images (generated by the Himawari-8 satellite [25]) of Kanto area in a day with a high fluctuation of PV power within the LFC time frame. Fig. 8(a) shows 2 GW fluctuation PV power in Kanto near noon time on 25th of August 2016. This was the highest regional fluctuation of PV power in the period studied. In Fig. 8(b), just the interval in which the fluctuation occurred is presented. In less than 3 minutes, the 1-minute averaged PV power output increased from 10.2 GW to 12.3 GW.

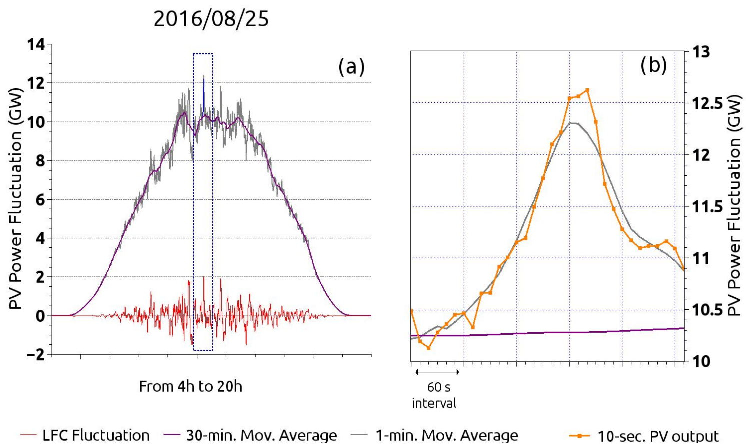

Figure 8- Example of a day (2016/08/25) with high PV power fluctuation within LFC time frame. Plot of daily PV power generation (a) and only of the one of the period in which the fluctuation occurred (b).

Comparing the 30-minute average PV power in Fig. 8(b), which is used as baseline, the total fluctuation reached 2 GW. In the same period, PV power fluctuations within GFC time frame, represented by the difference between the 10-second output and its 1-minute average, was small (less than 0.5 GW in the worst case). Such fluctuation of PV power in regional scale is related with the weather and atmospheric condition of the day in which it occurred. Fig. 9 shows the corresponding cloud conditions, according to satellite images, at the hour the fluctuations happened.

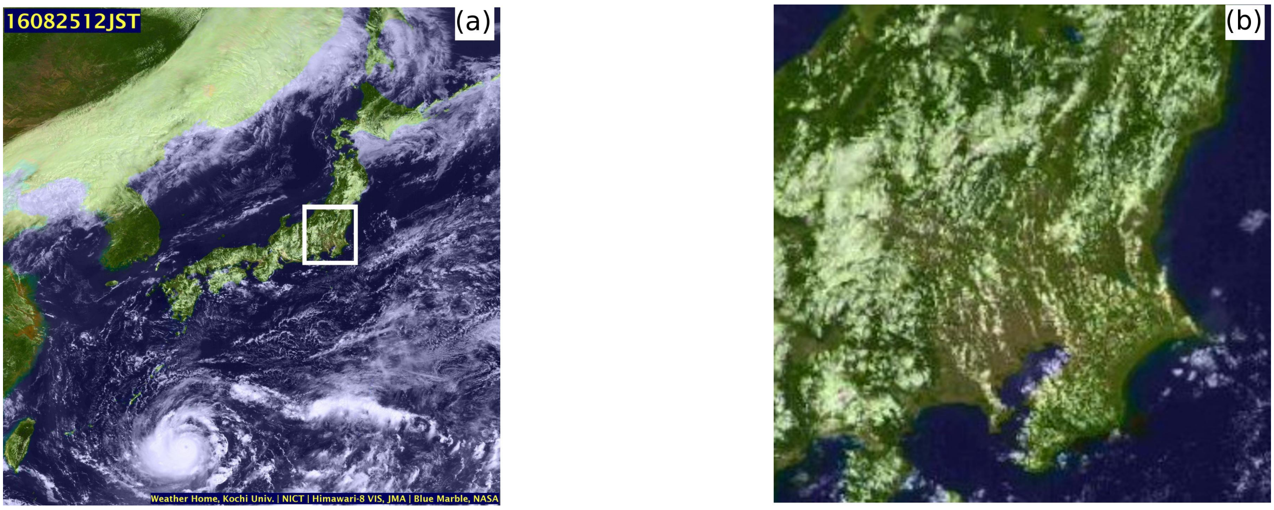

Figure 9- Satellite images of Japan surroundings (a) and Kanto area (b) at the hour of the PV power fluctuations in 25th of August 2016, presented in Fig. 9(b) (source: Kochi University [29]).

In this day, there was a typhoon approaching Japanese islands from the south. However, it is still too far to have a direct effect on the weather of Kanto. On the same day, there was a cold front moving from northwest to southeast direction, Fig. 9(a), and a zone of high pressure on the East of Kanto at the pacific ocean (not shown here). Considering still the usual high concentration of water vapor in summer, these conditions favored sparse clouds formation in most of the country. In Kanto area at the hour of the fluctuation, noon in Fig. 9(b), the day was mostly sunny with scattered clouds in the sky. The same Fig. 9(b) shows that in the areas surrounding Kanto, the conditions were different with more clouds. Looking at the registered weather for Kanto region in this day, it was a day with high temperatures and high humidity [26]. Under these conditions, most of the area received strong solar irradiance, which is intermittently blocked by passage of sparse clouds in the region at noon, causing the strong fluctuation noted in Fig. 8(b).

The highest fluctuation of PV power that occurred within the GFC related time frame happened in 19th of August 2016, shown in Fig. 10(a) and Fig. 10(b). On this day, the highest PV power fluctuation reached 1.1 GW.

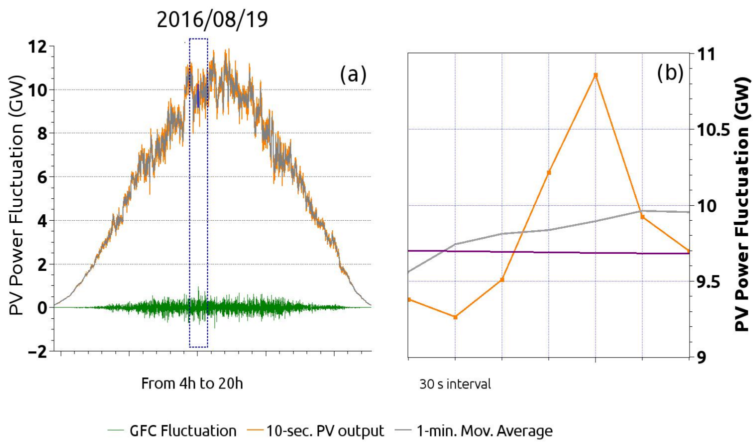

Figure 10- Example of a day with high PV power fluctuation within GFC time frame. Plot of daily PV power generation (a) and only of the period in which the fluctuation occurred (b).

Looking at Fig. 10(b), one can see that the fluctuation happened in less than 20 seconds. Moreover, as it happened in August 25th in Fig. 8, the regional PV power generation reached high values at noon time, more than 10 GW.

The satellite image of Japan on August 19th, in Fig. 11(a), indicates that there is a tropical depression east of the Japanese islands. Looking only at Kanto area at the time the fluctuation of PV power happened, the weather is mostly sunny with the exception of some border areas on the north and west.

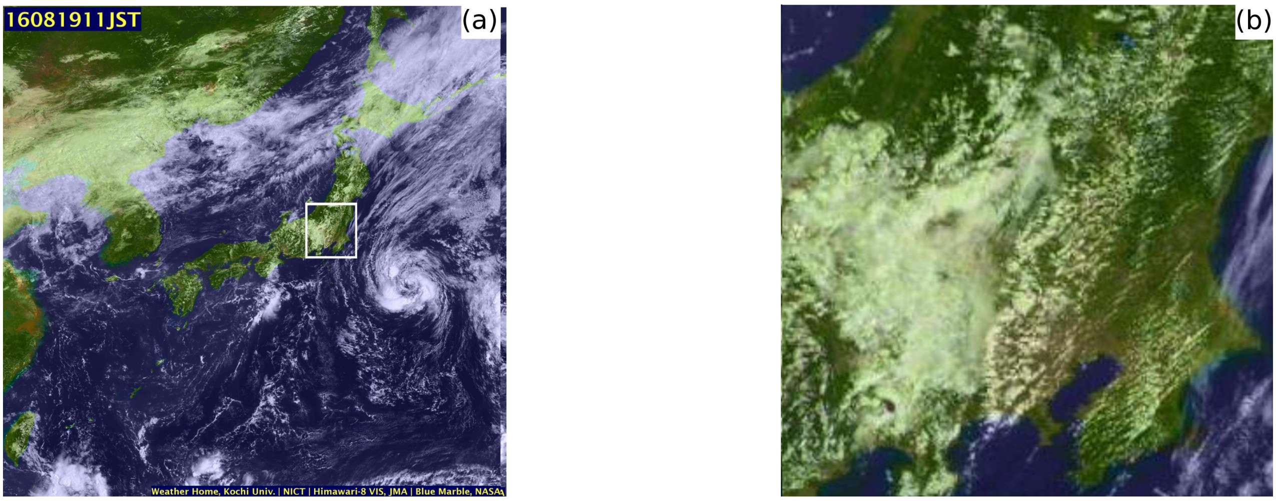

Figure 11- Satellite imaging of Japan surroundings (a) and Kanto area (b) at the hour of the PV power fluctuations on August 19th of 2016, presented in Fig. 11(b) (source: Kochi University [29]).

Surrounding areas, however, are covered with clouds (and there is some precipitation of rain on the west of Kanto). Overall, the characteristics are similar to those of August 25th, when the largest fluctuations within LFC time frame happened. Nevertheless, comparing Fig. 11(b) with Fig. 9(b), sparse clouds in Kanto area are different, with higher frequency of small clouds covering the region on August 19th than on August 25th. We infer that the passage of such kind of clouds in the area is the cause of the high frequency of the fluctuation of PV power noted in Fig. 10.

To show fluctuations that happened in different weather regime of those in Fig. 8 and Fig. 10, the last example in Fig. 12(a) is of a day during the rainy season. In this day, not only surges of PV as those presented in Fig. 8 and Fig. 10 happened, but also strong short-term drops of PV power generation. Furthermore, under such weather, regime fluctuations within both LFC and GFC time frames had high values. The corresponding satellite images for this day, June 14th, in Japan and in Kanto area are in Fig. 12(b) and Fig. 12(c).

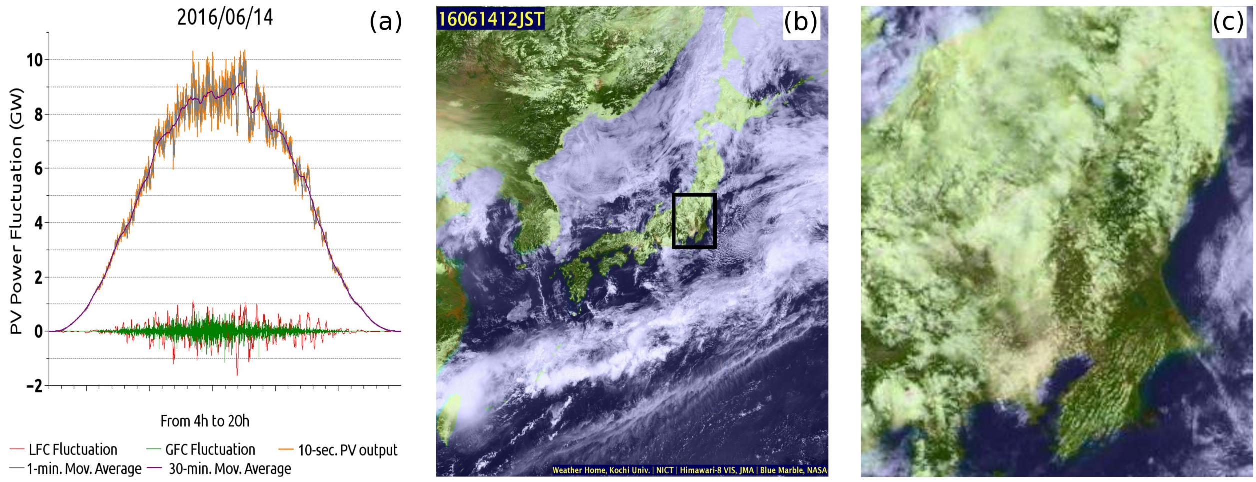

Figure 12- Example of a day with high fluctuations of PV power within LFC and GFC time frames (a), and corresponding satellite visible images of Japan (b) and Kanto area (c) at noon time of 14th of May 2016 (images' source: Kochi University [29]).

According to Fig. 12(c), in June 14th, there was a high level of nebulosity in the north and west parts of Kanto area. There were sparse clouds in the central and south parts of the area. According to the weather register of the Meteorological Society of Japan [27], [28], a stationary front, known in Japan as *baiu front*, bringing the rain season in 2016, started in the first half of June around Okinawa and progressed rapidly to the main island Honshu, bringing rain, high humidity, warm temperatures, and unstable weather. By June 14th, another stationary front extending from Okinawa on the south to the ocean near to the eastern area in Japan, with a low pressure zone at the east of Kanto, brought further atmospheric instabilities in the whole country. These instabilities caused the weather to be sunny with cloudy and sparse clouds intervals in Kanto area during the whole day, causing short-term fluctuations of PV power in the order of 1 GW.

5. Conclusions

In this study we analyzed the characteristics of short-term fluctuations of PV power generation in regional scale in Japan in a scenario of high penetration of PV on a power grid. We used 1 year of the most recent high resolution measured GHI data available in Japan with a method to convert them to regional PV power. Moreover, to provide a comprehensive analysis of the fluctuations, a methodology was proposed and applied to characterize the fluctuations on time frames of interest to power grid operators. Besides the statistical properties, the fluctuations were studied considering also the weather, seasonal, and power demand conditions in which they happened. Supporting examples, describing the specific weather conditions that caused extreme fluctuations, were also provided

The results showed a clear distinction between the regional PV power short-term fluctuations according to the time frames of primary and secondary regulation controls of frequency. Fluctuations occurring within the GFC time frame were smaller than those within LFC time frame. Their extreme values also had less dependence on the season than in LFC time frame related extreme fluctuations. Nevertheless, GFC time frame related fluctuations were stronger than LFC time frame related ones, presenting extreme values that reached almost 20 times their annual standard deviation, and that were up to 3 times higher than their 99th percentile related values. We were able to estimate that, for the case studied, the fluctuations were at most 5% of the average hourly power demand at the time in which they occurred, and that they can happen in different atmospheric conditions. Finally, we verified that the non-gaussian characteristics of the annual distribution of short-term fluctuations of PV power is also present in Japan. In this case, the distribution of the short-term fluctuations of PV power had a shape remarkably similar to the shape of a Laplacian distribution.

With the growing penetration of renewable energy systems in power grids around the world, understanding the effects that such systems exert on the operation of regional power systems will become vital to their stability. Thus, further analyses of the short-term fluctuations of the power of renewable energy systems in high penetration scenarios have to go beyond simply identifying statistical properties of related fluctuations, and also to evaluate them and their magnitude in the context of operation of the whole power system. With the analysis and methodology presented here, we give a step in this direction. Such methodology is of simple application and its use is not restricted to the specific characteristics of Japan. Thus, it can be used anywhere in the world where there is PV power output measurements in regional scale.

Acknowledgment

This work was funded by the “Demonstration Project of Forecast Technologies for Photovoltaic Generation” of the Ministry of Economy, Trade and Industry of Japan.

References

[1] IEA-PVPS, ‘IEA - TRENDS Report’, 2016. [Online]. Available: http://www.iea-pvps.org/index.php?id=256. [Accessed: 15-Feb-2017].

[2] J. Remund, C. Calhau, L. Perret, and Marcel, Davy, ‘Characterization of the spatio-temporal variations and ramp rates of solar radiation and PV’, IEA, IEA PVPS T14-05:2015, 2015.

[3] E. Wiemken, H. G. Beyer, W. Heydenreich, and K. Kiefer, ‘Power characteristics of PV ensembles: experiences from the combined power production of 100 grid connected PV systems distributed over the area of Germany’, Solar Energy, vol. 70, no. 6, pp. 513–518, 2001.

[4] K. Otani, J. Minowa, and K. Kurokawa, ‘Study on areal solar irradiance for analyzing areally-totalized PV systems’, Solar Energy Materials and Solar Cells, vol. 47, no. 1–4, pp. 281–288, 1997.

[5] W. T. Jewell and T. D. Unruh, ‘Limits on cloud-induced fluctuation in photovoltaic generation’, IEEE Transactions on Energy Conversion, vol. 5, no. 1, pp. 8–14, 1990.

[6] A. Murata, H. Yamaguchi, and K. Otani, ‘A method of estimating the output fluctuation of many photovoltaic power generation systems dispersed in a wide area’, Elect. Eng. Jpn., vol. 166, no. 4, pp. 9–19, 2009.

[7] A. Woyte, V. V. Thong, R. Belmans, and J. Nijs, ‘Voltage fluctuations on distribution level introduced by photovoltaic systems’, IEEE Transactions on Energy Conversion, vol. 21, no. 1, pp. 202–209, 2006.

[8] A. E. Curtright and J. Apt, ‘The character of power output from utility-scale photovoltaic systems’, Progress in Photovoltaics: Research and Applications, vol. 16, no. 3, pp. 241–247, 2008.

[9] M. Lave, J. Kleissl, and E. Arias-Castro, ‘High-frequency irradiance fluctuations and geographic smoothing’, Solar Energy, vol. 86, no. 8, pp. 2190–2199, Aug. 2012.

[10] T. E. Hoff, R. Perez, J. Kleissl, D. Renne, and J. Stein, ‘Reporting of irradiance modeling relative prediction errors’, Prog. Photovolt: Res. Appl., vol. 21, no. 7, pp. 1514–1519, 2013.

[11] S. J. Wellby and N. A. Engerer, ‘Categorizing the Meteorological Origins of Critical Ramp Events in Collective Photovoltaic Array Output’, J. Appl. Meteor. Climatol., vol. 55, no. 6, pp. 1323–1344, 2015.

[12] J. Marcos, L. Marroyo, E. Lorenzo, and M. García, ‘Smoothing of PV power fluctuations by geographical dispersion’, Prog. Photovolt: Res. Appl., vol. 20, no. 2, pp. 226–237, 2012.

[13] J. Marcos, L. Marroyo, E. Lorenzo, D. Alvira, and E. Izco, ‘Power output fluctuations in large scale pv plants: One year observations with one second resolution and a derived analytic model’, Prog. Photovolt: Res. Appl., vol. 19, no. 2, pp. 218–227, 2011.

[14] T. Kato, S. Kumazawa, Y. Suzuoki, N. Honda, M. Koaizawa, and S. Nishino, ‘Evaluation of long-cycle fluctuation of spatial average insolation in electric utility service area’, in 2012 IEEE Power and Energy Society General Meeting, pp. 1–6, 2012.

[15] H. Nagoya, S. Komami, and K. Ogimoto, ‘A Method for Presuming Total Output Fluctuation of Highly Penetrated Photovoltaic Generation Considering Mutual Smoothing Effect’, Elect. Eng. Jpn., vol. 186, no. 3, pp. 31–42, 2014.

[16] M. Anvari et al., ‘Short term fluctuations of wind and solar power systems’, New J. Phys., vol. 18, no. 6, pp. 1-14, 2016.

[17] T. Oozeki, J. Fonseca, T. Takashima, and K. Ogimoto, ‘Dataset of photovoltaic system output for power system analysis’, Technical Meeting on Metabolism Society and Environmental Systems, IEE Japan, vol. 2011, no. 15, pp. 1–5, 2011, ‘in Japanese’.

[18] Ministry of Land, Infrastructure, Transport and Tourism of Japan – National and Regional Police Bureau, ‘GISHP (Internet Service)’, [Online], Available: http://nlftp.mlit.go.jp/ , [Accessed: 24-Mar-2017], ‘in Japanese’.

[19] Japanese Institute of Irrigation and Drenage, ‘GIS Guide of Japanese Land and Waters’, [Online], Available: http://www.nngis.jp/login.php , [Accessed: 24-Mar-2017], ‘in Japanese’.

[20] Japan Statistics Bureau, ‘Portal Site of Official Statistics of Japan GL01010101’, [Online], Available: http://www.e-stat.go.jp/SG1/estat/eStatTopPortal.do , [Accessed: 24-Mar-2017].

[21] Japan Photovoltaic Energy Association - JPEA, ‘Heisei 28 JPEA Guidelines on Proper Identification of Photovoltaic Related Products and Services‘, Available: http://jpea.gr.jp/pdf/t16072201.pdf , [Accessed: 24-Mar-2017], 2016, ‘in Japanese’.
[22] NEDO, ‘White Paper on Renewable Energy Technologies - 2nd Edition, White Paper, Japan, 2014, ‘in Japanese’.
[23] Institute of Electrical Engineers of Japan - IEEJ, ‘Load-Frequency Control in Normal and Anomalous Conditions’, IEEJ Technical Report, Japan, n. 869, 2002, ‘in Japanese’.
[24] C. Urabe T., T. Saito, K. Kataoka, T. Ikegami, and K. Ogimoto, ‘Analysis of Short-Period Fluctuation of Wind Power Output’, in Proceedings of the Twenty-Eighth Annual Conference of Power & Energy Society, Kyushu, vol. 6–210, pp. 345–346, 2016, Japan, ‘in Japanese’.
[25] K. Bessho et al., ‘An Introduction to Himawari-8/9— Japan’s New-Generation Geostationary Meteorological Satellites’, Journal of the Meteorological Society of Japan. Ser. II, vol. 94, no. 2, pp. 151–183, 2016.
[26] Japan Meteorological Association, ‘Past Weather Information’, Tenki.jp. [Online]. Available: http://www.tenki.jp/past/ [Accessed: 24-Mar-2017], ‘in Japanese’.
[27] METSOC, ‘Weather in Japan on June of 2016’, Tenki, vol. 63, no. 8, p. 592, 2016, ‘in Japanese’.
[28] METSOC, ‘Daily Weather Map in Japan on June of 2016’, Tenki, vol. 63, no. 8, p. 595, ‘in Japanese’.
[29] Kochi University, ‘Weather Information’, [Online], Available: (http://weather.is.kochi-u.ac.jp/ , [Accessed: 24-Mar-2017], ‘in Japanese’.